Current Biology, Volume *23*
Supplemental Information

Selective Attention in an Insect Visual Neuron

Steven D. Wiederman and David C. O'Carroll

Supplemental Figures

Figure S1, Linked to Figure 1.
CSTMD1's morphology and receptive field maps for different sized features used in the main figures.

Figure S2, Linked to Figure 3.
Internal noise in responses to repetition of the same stimuli.

Figure S3, Linked to Figure 4.
Percentage time tracking each target and additional error analysis at 5° and 10° target separations.

Supplemental Experimental Procedures

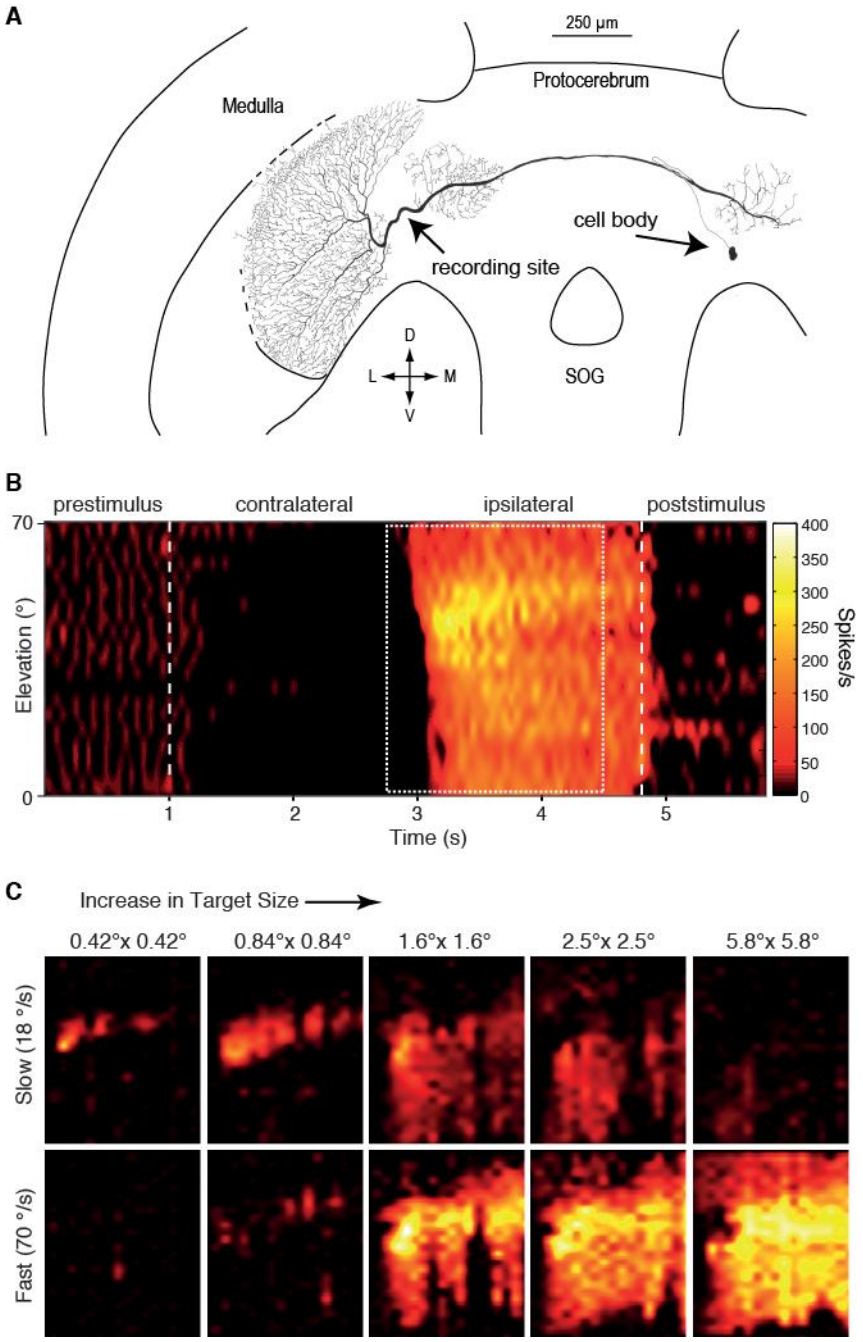

Figure S1, Linked to Figure 1. CSTMD1's Receptive Field Is Dependent on Target Size and Velocity

(A) CSTMD1's morphology reconstructed from a Lucifer Yellow fill. Major dendritic input is in the ipsilateral mid-brain (relative to the cell body) and there is a large output arborisation in the contralateral optic lobe. A second contralateral arborization co-localizes with the input dendrites of the mirror symmetric CSTMD1.

(B) A 2-d (time versus elevation) receptive field map of CSTMD1 in response to small targets (1.25°x1.25°) scanned horizontally across the display at 42°/s and at 21 different elevations. The time during which the target was present on the display is indicated by the vertical white dashed (long) lines. As a target traverses the contralateral hemifield, spike rate is inhibited to below spontaneous. The neuron

is then strongly excited when the target crosses the midline into the ipsilateral hemifield, with responses gradually weakening towards the periphery, until the target leaves the stimulus display. In the post-stimulus period, CSTMD1 exhibits spike rate suppression due to a post-excitatory rebound.
(C) In a long, single CSTMD1 recording, we repeated vertical receptive field scans at varying target sizes (randomly interleaved) and at slow (18°/s) and fast (70°/s) velocities from an ipsilateral subregion of the overall receptive field (as illustrated by dotted lines in A). As target size increases, maximum responses shift towards the periphery. CSTMD1 is both size and velocity tuned and neuronal output represents a confounded interplay between target position, size and velocity.

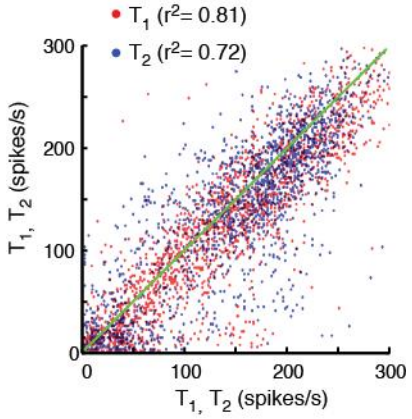

Figure S2, Linked to Figure 3. Correlation of Single Target Responses from Repeated Trials Reveal the Level of Neuronal Variability
Trial to trial variability (neuronal noise) degrades the correlation between the response for any single 25ms bin from the instantaneous spike frequency plot for either T_1 or T_2 and that for the equivalent bin in a subsequent repetition of an identical stimulus. The scatter plots show data pooled across the same set of 4 combinations of target pairs as in Figure 3: Low (0.56) and high (1.0) contrast, small (1.25° square) and large (2.5° square), all at 20° separation, for T_1 (red points) and T_1 (blue points). The mean correlation of T_1 with T_1 is stronger ($r^2 = 0.81$) than for T_2 with T_2 ($r^2 = 0.72$), with an overall average r^2 of 0.76. This may reflect greater sensitivity and reliability in the T_1 response, since the latter traverses the frontal hotspot of the receptive field (Figure 1), where the ommatidial facet lenses of the eye are larger and acuity is higher. Although the CSTMD1 receptive field is stable and repeatable over time (Figure 1D,F), we note that because individual trials of T_1, T_2 and Pair for each combination of target size, contrast and separation were presented in randomized blocks, the average time between an identical T_1 or T_2 stimulus is substantially longer than between the corresponding T_1, T_2 and Pair within a block. Hence longer-term drift in response over time (e.g. due to habituation) may contribute additional noise to this data compared with the correlations from within the blocks for the same data set shown in Figure 3.

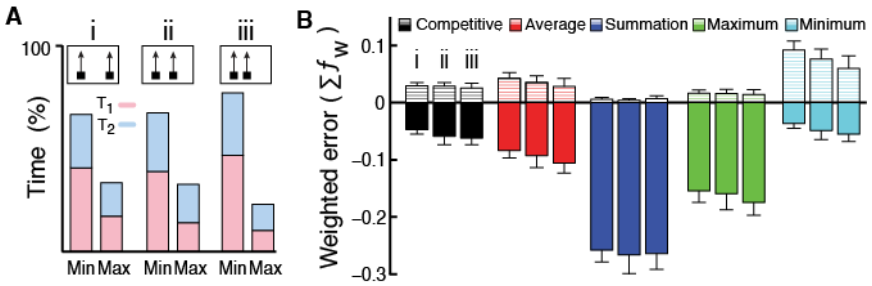

Figure S3, Linked to Figure 4. Competitive Selection Is the Most Accurate Model over a Range of Target Sizes, Contrasts, and Separations
(A) Paired response tracked T_1 more than T_2 (58:42) and this was more likely the minimum of T_1 and T_2 responses. This bias increased at smaller target separations (20°, 10°, 5°).
(B) Over 11 dragonflies, we repeated T_1, T_2 and Pair experiments at 20° separation (n=72), 10° separation (n=40) and 5° separation (n=40). Weighted errors (mean ± 95%CI) were similar under three target separations, trending to more negative errors as separation decreased.

Supplemental Experimental Procedures

We inserted 2M KCl intracellular electrodes (80-120 MΩ) into the brain of immobilized *Hemicordulia tau* (11, either sex). We identified CSTMD1 from its characteristic receptive field (37 horizontal and 21 vertical target scans on a 120 Hz HD LCD monitor, 100°x80° viewing extent). For full details of these methods, see [13].

For our experimental protocol, T_1 moved through the receptive field hotspot and T_2 was located either 5°, 10° or 20° to the right. Dark targets of low (0.56) or high (1.0) contrast ($I_{difference} / I_{background}$) were drifted vertically (42°/s) on a white background (315 $Cd.m^{-2}$) at either small (1.25°x1.25°) or large (2.5°x2.5°) sizes. T_1, T_2 and Pair, of varying sizes and contrasts, were all randomly interleaved (rest period of 14-17s). Repeated single target controls revealed no evidence of habituation.

We binned (25ms) the spike responses and lightly filtered (Savitzky-Golay [42], 2°, 7-span) the peri-stimulus time histograms. Data for further analysis were taken from bins where stimuli were within the receptive field, determined via an inclusion criterion of T_1 or T_2 being above a threshold of 1.5 x standard deviation of the spontaneous activity for each cell. We represented neuronal saturation in the *Summation* model with a hyperbolic tangent function with the saturation level set at 99^{th} percentile of responses for that set of trials.
Over 11 dragonflies, we repeated T_1, T_2 and Pair experiments at 20° separation (n=72), 10° separation (n=40) and 5° separation (n=40). This pooled data was separated into each target size and contrast condition (n = 18, 10 and 10 respectively). For statistical comparison, we examined unsigned errors of the pooled data (at each separation) with 1 way ANOVA and Dunnett's post hoc test (competitive selection as the reference group). All error bars represent mean ± 95%CI. Effect sizes between models are reported as Cohen's d ($\sigma_{average}$) ± 95%CI.